JOURNAL OF CATALYSIS 130, 220–237 (1991)

Surface Structure and Reactivity of V–Ti–O Catalysts Prepared by Solid-State Reaction

1. Formation of a V^{IV} Interacting Layer

G. CENTI,* E. GIAMELLO,† D. PINELLI,* AND F. TRIFIRÓ*

*Department of Industrial Chemistry and Materials, V.le Risorgimento 4, 40136 Bologna, Italy; and †Department of Inorg., Phys.-Chem. and Materials, v.P. Giuria 9, 10125 Torino, Italy

Received May 9, 1990; revised January 21, 1990

The solid-state interaction between V_2O_5 and TiO_2 in the 700–800 K range of temperatures gives rise to the formation of V^{IV} sites even in the absence of reducing agents. A V^{IV} interacting layer covering the entire surface of TiO_2 anatase may be created in the absence of any indication of partial transformation to the rutile phase. The nature, amount, and distribution of these V^{IV} sites are characterized by means of titration combined with selective extraction, reactivity measurements in *o*-xylene oxidation, evaluation of redox properties, and by XRD, XPS, and ESR analyses. The amount of V^{IV} depends on the crystallographic nature (anatase or rutile) and surface area of the TiO_2 and on the conditions (temperature, time, and type of atmosphere) of the heat treatment. In the anatase sample the V^{IV} sites can be reduced to V^{III}, but not oxidized to V^{V} due to the strong interaction with the titania surface. In rutile samples part of the V^{IV} may be reduced to V^{III}, but also oxidized to V^{V}. The remaining V^{IV} sites are present in solid solution in the rutile matrix and are not accessible to redox reagents. The model of a V^{IV}-modified TiO_2 (anatase) surface is discussed with reference to the problem of surface diffusion of vanadium species on the anatase surface. In TiO_2 (rutile)-based samples, due to the competition of the migration of vanadium ions toward the bulk of the rutile with respect to surface diffusion, V_2O_4-like islands form that are coherently intergrown into the main rutile TiO_2 matrix.

INTRODUCTION

Vanadium–titanium oxides constitute a well-known catalytic system showing specific support-active phase interaction. The catalytic behavior of vanadium-oxide supported on TiO_2 is enhanced in comparison with its being supported on other oxides such as SiO_2 or Al_2O_3 (*1–5*). Several interpretations have been advanced in the literature to explain this specific influence of the TiO_2 surface on V reactivity. The presence of a crystallographic fit between crystalline planes of V_2O_5 and TiO_2 has been hypothesized to lead to a *spreading* of V-oxide on the surface of the support to form a monolayer with a preferential exposition of a specific crystalline plane (*6–8*). Other authors believe, on the contrary, that an amorphous disordered multilayer of V_2O_5 is present on the whole surface (*9–12*), on specific edges (*13*), or that paracrystalline "tower-like" V_2O_5 (*5, 14*) or coherent further layers (*11*) accrue on the first layer. According to Hausinger *et al.* (*15*), depending on the type of preparation and the presence of water, vanadia may interact weakly or strongly with TiO_2 leading to different surface structures of vanadium oxide: small packages of a V_2O_5 layer on the (101) plane of TiO_2 in the first case and polyvanadate in the second case. Finally, according to another research group (*16, 17*), the specific interaction of V with the TiO_2 surface forms a tetrahedral dioxo-V-species with enhanced catalytic properties in comparison with octahedral V in V_2O_5.

These different interpretations all have one aspect in common: only one single-monolayer species of V^{V} is thought to be

0021-9517/91 $3.00

present on TiO_2 surface. In previous work (*18–23*), however, we have shown the greater complexity of the surface situation of V-oxide species on TiO_2, evidencing, in particular, (i) the presence of V^{IV} as well as V^V on the surface of anatase titanium oxide and (ii) the presence of three or more V species characterized by different solubility in extraction media. The presence of both V^V and V^{IV} ions on the surface of TiO_2 agrees with the results of Fierro *et al.* (*24*) and Rusiecka *et al.* (*25*). However, questions remain about their nature and surface localization on the TiO_2 surface and relationship with the active phase. Our previous works using impregnation (*20*) or grafting (*19*) techniques on a high surface area TiO_2, or coprecipitation methods (*18, 22, 23*) did not allow clear answers. We have, therefore, adopted the method of solid-state reaction between V_2O_5 and TiO_2. This preparation method allows better and easier characterization of the nature and stages of formation of V species (*21*) and, in addition, is suitable for the synthesis of industrial V–Ti–O catalysts for *o*-xylene oxidation to phthalic anhydride (*26*). Therefore, despite its inherent simplicity, this method of preparation leads to a catalytic system very representative of the surface situation of V-oxide active species on TiO_2.

The mechanical mixture of V_2O_5 and TiO_2 is (a) first calcined in air at 773 K and (b) then treated in long-run catalytic tests in *o*-xylene oxidation. As previously shown (*21*), the catalytic behavior evolves during the latter treatment and both the activity and selectivity to phthalic anhydride increase indicating the formation of the active phase using this procedure of preparation of the catalyst. On the contrary, a V^{IV} strongly interacting species forms mainly during the first stage (a), at temperatures lower than that necessary for the V-catalyzed transformation of TiO_2 from anatase to rutile (*21*), and is still present after long-run treatments. It is thus possible to distinguish and characterize the two stages of transformation of V-oxide on TiO_2. We have thus performed a systematic characterization of V-oxide species formed on TiO_2 anatase and rutile surfaces during the heating and treatments in the reaction atmosphere of *o*-xylene oxidation. In this first paper we report data on the formation and characterization of the V^{IV} species formed by solid-state interaction of V_2O_5 with anatase or rutile TiO_2 during the first stage heat treatment. The evolution of the catalyst during *o*-xylene oxidation treatments, the characterization of the active phase for phthalic anhydride synthesis, and the redox stability of the V-oxide species on the different structures of TiO_2 are reported in the following article.

EXPERIMENTAL

Catalyst Preparation

The catalysts were prepared by mechanical mixing of TiO_2 and V_2O_5 (Carlo Erba reagent grade). Generally, 7.7 wt% V_2O_5 was used, an amount typical for industrial preparations. Anatase and rutile prepared by $TiCl_4$ hydrolysis were used in order to obtain highly pure TiO_2 supports and to exclude interferences from doping. By a suitable control of the temperature of calcination in the 670–970 K range and of the time of treatment it is possible to control the surface area of TiO_2. For example, the calcination of the titanium hydrogel precursor of TiO_2 anatase at 823, 898, and 923 K for 24 h gives rise to pure TiO_2 anatase samples with the following surface areas: 64, 17, and 12 m^2/g, respectively. Temperatures of calcination about 100 K lower are required to obtain similar surface areas of TiO_2 rutile, starting from the corresponding Ti-hydrogel precursor obtained by precipitation at pH lower than 1.5. After mixing and gentle grinding (1 min, in order to have good mixing but at the same time avoid mechanicochemical alterations of the samples), the powder was calcined in an oven at 773 K for 16 h or longer in a static air atmosphere. Special alternative heat treatments in controlled atmosphere (see text) were made in a tubular reactor (reagent flow, 1.8 l h^{-1}) on the powder after the mixing procedure. Samples

subjected to different grinding times (in the 0–1800 s range) before calcination did not show appreciable differences in the amount of V^{IV} determined by chemical analyses. Alternative samples for specific tests (see text) were prepared by mechanical mixing of V_2O_5 with the titanium hydrogel precursors of TiO_2 anatase or rutile and subsequent calcination at 773 K.

Catalytic Tests

The catalysts were tested in a conventional laboratory apparatus with a tubular fixed-bed reactor working at atmospheric pressure and on-line gas chromatographic analyses of reagent and product compositions (*22, 23*). The standard reactant composition was 1.5% *o*-xylene, 20.5% O_2, and 78% N_2. The catalyst (0.52 g) was loaded as grains (0.250–0.420 mm). A thermocouple, placed in the middle of the catalyst bed, was used to verify that the axial temperature profile was within 2–3 K.

Chemical Analysis

The samples (about 0.5 g) were moistened at room temperature (RT) with 50 ml of a dilute (4 *M*) H_2SO_4 solution or with an ammonia solution (4 *M*) for 15 min under stirring and then filtered. The amount of vanadium was determined separately in the filtered solution and in the residual sample dissolved in boiling concentrated H_2SO_4 (16 *M*). The total amounts and the valence state of vanadium were determined by a titrimetric method as previously reported (*20–23, 27*).

The vanadium species extracted by the RT dilute sulphuric acid or ammonia solution are hereinafter, called *soluble* or *weakly interacting* species, whereas the remaining species determined after dissolving the residue are called *insoluble* or *strongly interacting* species. Special reference tests were designed to verify the correctness of the extraction and chemical analysis procedure: (i) analysis of the samples before calcination, (ii) tests of solubility and of chemical analyses on pure V and Ti oxides, (iii) tests with different extraction conditions (time, concentration) and determination by atomic absorption of the amounts of V and Ti solubilized, (iv) tests to verify the stability of valence states of vanadium in the extracted solution or during the dissolution procedure. Moreover, the coincidence of the results of chemical analysis with those of reduction/reoxidation cycles in a thermogravimetric apparatus was verified in order to assess the validity of the procedures for extraction and chemical analyses.

Characterization

X-ray diffraction patterns (XRD) (powder technique) were obtained using Ni-filtered Cu$K\alpha$ radiation and a Philips computer controlled instrument. Interplane spacings were collected at 2θ increments of 0.01°. Cell parameters were estimated by a least-squares method and using the eight most intense reflections of the rutile phase.

Surface areas were determined using the BET method and a Carlo Erba Sorptomatic instrument.

The tests of reducibility/reoxidability of V^{IV} were made isothermically at 673 K in a thermogravimetric apparatus (Perkin–Elmer TG2) using a flow of 2% H_2 in helium or of 20% O_2 in nitrogen, respectively. Additional tests of reoxidability of V^{IV} were made by static calcination at 673 K (3 h) and chemical analysis of the valence state of vanadium.

EPR spectra were recorded at room temperature and liquid nitrogen temperature (77 K) using an *X*-band Varian E109 spectrometer. A special cell containing EPR tubes and suitable connections with conventional gas manipulation and evacuation ramps was employed. In all samples employed for EPR experiments, the V^V soluble species were removed by selective chemical extraction using NH_3 or dilute H_2SO_4 solutions in order to improve the characterization of the V^{IV} species. Varian pitch ($g = 2.0029$) was used

for g value calibration. The spin-Hamiltonian parameters (g, A) were calculated taking into account the second-order effects, by means of a suitable computer program.

X-ray photoelectron spectroscopy (XPS) results were obtained using a VG ESCA LAB instrument equipped with an Al anode. Binding energies were determined using the O_{1s} peak at 529.8 eV as a reference to correct charge effect. The O_{1s} peak was used to correct the charge effect instead of C_{1s} peak, because, especially in the samples after the catalytic tests, the C_{1s} peak is very broad due to the presence of several partially overlapping peaks related to the presence of both contaminant molecules and adsorbed species (especially aromatics) remained on the surface after the catalytic tests. The sputtering of the surface was realized using a Ne^+ ion gun after calibration of the amount of layers removed with time and of the sputtering yield of V and Ti.

RESULTS

Characterization by Chemical Analysis

The method of chemical analysis combined with extraction of vanadium species in ammonia or dilute sulphuric acid solution allows the distinction between some different types of vanadium species: (a) a V^V species, such as V_2O_5, soluble in the ammonia or sulphuric acid solution; (b) a V^{IV} species soluble in the sulphuric acid solution only; and (c) a V^V species or (d) a V^{IV} species that cannot be extracted using the ammonia or dilute sulphuric acid solutions, but that can be determined after complete dissolution of the sample. In addition to these two species, the presence of V^{III} species, if any, may also be determined by the combined titration method we use.

In all cases after calcination of the mechanical mixture of TiO_2 and V_2O_5 only species (a) and (d) were found in the samples. We report here the effect of some reaction variables on the amount of species (d) (*non-soluble* V^{IV}).

Effect of the surface area. The effect of the surface area of TiO_2 on the amount of non-soluble V^{IV} formed by calcination under a flow of air of the mechanical mixture of V_2O_5 and TiO_2 is shown in Fig. 1 for anatase and rutile samples. For the sake of comparison, the amount of V^{IV} determined by chemical analyses is reported as percentage by weight of equivalent moles of $VO_{2.5}$. In all cases the composition of the starting sample is 7.7 wt% V_2O_5 and 92.3 wt% TiO_2. A reference theoretical line corresponding to the value for a monolayer of vanadium oxide on the whole TiO_2 surface, assuming, according to Bond *et al.* (*4, 5*), a value of about 0.1 wt% of V_2O_5 per square meter of TiO_2 surface is also reported.

It is shown that the amount of V^{IV} is approximately equivalent to the reference monolayer for low surface area anatase samples (10 m^2/g or below), but much less in samples with a higher surface area (Fig. 1). A higher amount of V^{IV} is found in all the TiO_2 rutile samples. The effect is particularly evident for the higher surface area samples.

Role of the atmosphere of calcination. The nature of the calcination atmosphere has a considerable effect on the amount of non-soluble V^{IV}. Figure 1 reports the effect of the presence of a reducing agent during the heat treatment [flow of 10% NH_3 in air (773 K, 24 h)]. This treatment was followed by calcination. In fact, the V^{IV} which does not directly interact with the TiO_2 surface, may be easily reoxidized to V^V (*18*) and thus the consecutive calcination of the sample may better show which part of the V^{IV} produced during the reduction step has interacted with the TiO_2 surface.

The heating in the presence of a reducing agent greatly increases the amount of non-soluble V^{IV}. In the case of the anatase sample with low surface area (11 m^2/g) the increase is relatively limited until the amount equivalent to the monolayer is reached. For higher surface areas, the increase is more sensible, but the amount still remains below the reference monolayer. Also for the rutile sample, the treatment causes an increase in

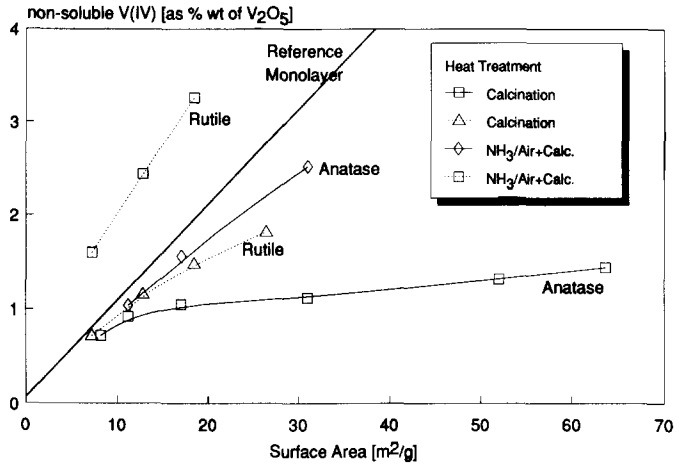

FIG. 1. Amount of non-soluble V^{IV} (as wt% of equivalent V_2O_5) determined by chemical analysis of mechanical mixtures of V_2O_5 and TiO_2 (anatase or rutile, prepared by $TiCl_4$ hydrolysis) after different heat treatments at 773 K (24 h).

the amount of the V^{IV}. However, in this case the amount of V^{IV} is higher (about twice) than the reference monolayer.

Similar effect are observed when the treatment is performed in vacuum (773 K, 10^{-3} Torr). In vacuum there is a spontaneous reduction of most of the V^{V} which is easily reoxidized during the consecutive heat treatment in air. The final amount of V^{IV} is very similar to that found after treatment in a flow of ammonia/air and subsequent calcination. Also the calcination in a flow of air/steam increases the amount of non-soluble V^{IV}, indicating the promoting effect of water on the process of formation of non-soluble V^{IV} species by solid-state interaction between V_2O_5 and TiO_2.

Role of the nature of TiO_2. The presence of impurities and the degree of hydroxylation of the surface have a considerable effect on the amount of V^{IV}. Table 1 compares the amount of V^{IV} determined after calcination of the mechanical mixture of V_2O_5 and TiO_2 using commercial TiO_2 samples (from Degussa and from Tioxide—samples C and D, respectively) with that obtained using a TiO_2 sample prepared by hydrolysis of $TiCl_4$ and subsequent calcination in order to obtain a highly pure titanium-oxide surface (sample B). All samples have comparable surface area (around 18 m^2/g). The main impurities in the Tioxide sample are 0.29% SO_3, 0.07% P_2O_5, and 0.01% K_2O and those of the Degussa sample are 0.04% P_2O_5 and 0.03% K_2O.

It is shown that the greater amount of V^{IV} is obtained with the highly pure TiO_2 prepared by hydrolysis of $TiCl_4$. Surface impurities may thus inhibit the amount of non-soluble V^{IV} species. The amount of surface hydroxyl groups also affects the amount of V^{IV} (Table 1). When a mechanical mixture of V_2O_5 with the oxyhydrated precursor of TiO_2 anatase (*18, 27*) (sample A—the oxyhydrate was prepared by simply drying (423 K) the precipitate obtained by $TiCl_4$ hydrolysis at controlled pH (*27*)) is directly calcined, a greater amount of non-soluble V^{IV} is obtained. In this case, the sample is highly hydroxylated and the amount of V^{IV} is equivalent to the value of the reference monolayer.

Effect of the temperature and time of calcination. The effect of the calcination temperature on the formation of non-soluble VIV is shown in Fig. 2 for an anatase sample with a surface area of 9.8 m^2/g, the most interesting for catalytic applications in the

TABLE 1

Amount of Non-soluble V^{IV} (as wt% of Equivalent V_2O_5) Determined by Chemical Analysis as a Function of the Nature of Starting TiO_2 and of the Type of Treatment (See Also Text)

Type of TiO_2 (see text)	Sample	Surface area, (m^2/g)	Type of treatment	Non-soluble V^{IV} (wt% of equivalent V_2O_5)
Ti-oxyhydrate (precursor of TiO_2 anatase)	A	20.3	Calcination[b]	1.81
TiO_2 Anatase (by $TiCl_4$ hydrolysis)[a]	B	18.1	Calcination[b]	1.09
TiO_2 Anatase (Degussa)	C	17.8	Calcination[b]	0.89
TiO_2 Anatase (Ti-oxide)	D	18.4	Calcination[b]	0.61
TiO_2 Anatase (by $TiCl_4$ hydrolysis)[a]	E	9.8	Calcination[b]	0.79
TiO_2 Anatase (by $TiCl_4$ hydrolysis)[a]	E	9.8	*o*-Xylene oxidation (24 h)	0.90
TiO_2 Anatase (by $TiCl_4$ hydrolysis)[a]	E	9.8	*o*-Xylene oxidation (500 h)	0.95
TiO_2 Rutile (by $TiCl_4$ hydrolysis)[a]	F	8.7	Calcination[b]	0.80
TiO_2 Rutile (by $TiCl_4$ hydrolysis)[a]	F	8.7	*o*-Xylene oxidation (24 h)	1.95
TiO_2 Rutile (by $TiCl_4$ hydrolysis)[a]	F	8.7	*o*-Xylene oxidation (500 h)	3.79

[a] By $TiCl_4$ hydrolysis and subsequent calcination (see text).
[b] 773 K, 24 h.

selective conversion of *o*-xylene to phthalic anhydride. The formation of non-soluble V^{IV} species by solid-state interaction of V_2O_5 and TiO_2 starts at temperatures in the range of 573–673 K. No further sensible increase can be observed with increasing temperature up to 773 K. For the entire range of calcination temperatures no evidence for the formation of the rutile phase is observed by X-ray diffraction analysis. The amount of non-soluble V^{IV} increases continuously for an anatase sample during the first 24 h of calcination, whereas further heat treatment produces only a very limited increase in the amount of V^{IV}.

Comparison with a heat treatment in a flow of o-xylene/air. Amounts of non-soluble V^{IV} comparable to those previously discussed are found after catalytic tests in *o*-xylene oxidation. Summarized in Table 1 are the main results. For an anatase sample, even after long-term catalytic tests (500 h), an amount of V^{IV} analogous to that found after short-term catalytic tests (24 h) or after calcination is found. In the case of rutile samples, on the contrary, a sensible increase in the case of catalytic tests is observed. After long-term catalytic tests a limiting value of about 3.8 wt% of equivalent V_2O_5 is reached. A parallel contraction of the rutile cell volume is observed by X-ray diffraction analysis. The results are reported in Table 2. No change in the X-ray diffrac-

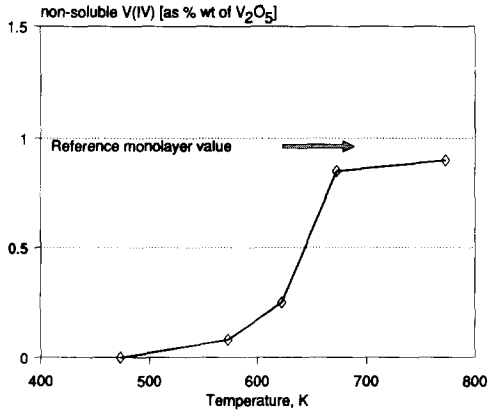

FIG. 2. Effect of the temperature of calcination of mechanical mixtures of V_2O_5 and TiO_2 (anatase, 9.8 m^2/g) on the amount of non-soluble V^{IV} determined by chemical analysis.

TABLE 2

Lattice Parameters for the Rutile Phase from a V_2O_5/TiO_2 (Rutile) Mechanical Mixture after Heat Treatments

Heat treatment (673 K)	*a* (Å)	*c* (Å)	Cell volume (Å)^3
Before	4.5955	2.9595	62.50
Air	4.5942	2.9592	62.46
Xylene/Air (24 h)	4.5924	2.9592	62.41
Xylene/Air (500 h)	4.5887	2.9591	62.31

tion pattern and in the cell volume is observed for anatase samples and also no diffraction lines due to the rutile phase appear.

Reactivity of Interacting V^{IV} Species

Flow reactor studies. The presence, reactivity, and distribution of interacting V^{IV} species in anatase and rutile samples were characterized using the *o*-xylene conversion to phthalic anhydride as a test reaction. Catalysts were pretreated using the washing procedure with dilute sulphuric acid solution to remove other vanadium species. As previously shown, in fact, using this procedure it is possible to solubilize the V^{V} and V^{IV} non-interacting species and thus to evaluate the influence on the catalytic behavior of a titania surface of the residual V^{IV} interacting species only.

The possible interference of the solubilization procedure on the reactivity of the TiO_2 surface was verified by testing samples treated with an ammonia solution or with the dilute sulphuric acid solution. The coincidence of the catalytic results indicates that the reactivity of the surface is not influenced by the solubilization procedure, i.e., for example, by residual sulphate species on the surface. The results obtained after different pretreatments are reported in Fig. 3. TiO_2 anatase and rutile samples with surface areas of 9.6 m^2/g and 8.9 m^2/g, respectively, were used as starting samples, because these surface areas are similar to those of industrial $V–TiO_2$ catalysts. The following three distinct types of treatments prior to the catalytic tests were made: (i) mechanical mixture, calcination and extraction (sample b); (ii) mechanical mixture, stream of *o*-xylene and air for 5 h at 623 K, and extraction (sample c); (iii) mechanical mixture, stream of *o*-xylene and air for 500 h, and extraction (sample d).

TiO_2 anatase and rutile surfaces not modified by V^{IV} (samples a in Fig. 3) exhibit very low activity in *o*-xylene oxidation and no selectivity at all in phthalic anhydride formation. A considerable increase in the activity in *o*-xylene oxidation for both anatase

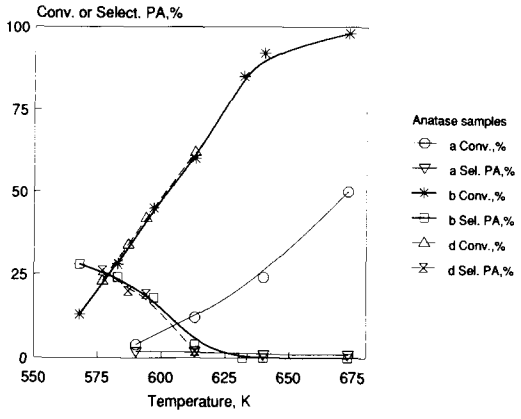

FIG. 3. Comparison of the catalytic behavior of mechanical mixtures of V_2O_5 and TiO_2 anatase (9.8 m^2/g after different pretreatments: (b) calcination at 773 K, (c) catalytic tests in *o*-xylene oxidation (5 h of time-on-stream), (d) catalytic tests in *o*-xylene oxidation (500 h of time-on-stream) with respect to the catalytic behavior of pure TiO_2 samples (a). Before the catalytic tests, soluble V species were removed by extraction (see text).

and rutile samples is noted when the mechanical mixtures of V_2O_5 and TiO_2 are calcined at 773 K and then washed (samples b). The activities of the two samples are comparable and in both cases the formation of phthalic anhydride is observed. The selectivity of the rutile sample, however, is slightly higher (about 35–40%), although below that of $V-TiO_2$ samples for which no washing treatment was made (*21*). Therefore, the presence of V^{IV} sites on the surface of TiO_2 enhances its reactivity toward *o*-xylene selective oxidation.

The tests of surface reactivity on samples c and d evidence a fundamental difference in the redox nature and stability of V^{IV} sites on anatase and rutile surfaces. The catalytic behavior of the anatase samples after pretreatment in an *o*-xylene/air stream (samples d) is analogous to that of the sample after calcination (sample b) and furthermore is constant with time-on-stream.

In rutile samples, on the contrary, an evolution of the catalytic behavior is observed (Fig. 4) which depends on the type of pretreatment. If the sample was pretreated for

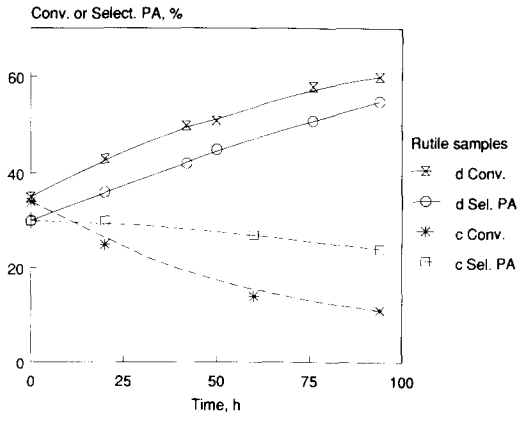

FIG. 4. Time evolution of the catalytic behavior in *o*-xylene oxidation of mechanical mixtures of V_2O_5 and TiO_2 (rutile, 8.9 m^2/g) after different pretreatments: (c) catalytic tests in *o*-xylene oxidation (5 h of time-on-stream), (d) catalytic tests in *o*-xylene oxidation (500 h of time-on-stream).

only a short time (sample c) and the amount of interacting V^{IV} is relatively low (less than 1 wt%—see Table I), the catalytic behavior worsens with time on stream (Fig. 4), whereas it improves in the case of catalysts pretreated for a long time (sample d) having a higher amount of interacting V^{IV} (about 3.8 wt%).

It should be noted that in the rutile sample d a partial oxidation of V^{IV} to V^{V} after 100 h of time-on-stream is observed and that the amount of V^{IV} in this sample is around the solubility limit. In sample c, on the contrary, due to a lower amount of V^{IV}, diffusion into the bulk of the rutile phase and formation of a solid solution (as indicated by the contraction of cell volume shown by XRD analysis—Table 2) occur. This effect decreases the amount of V^{IV} on the surface with a worsening of the catalytic behavior. Higher amounts of V^{IV} in rutile sample d prevent this effect and reoxidation of surface V^{IV} sites to V^{V} takes place with enhancement of the catalytic behavior.

Thermogravimetric redox studies. The differences in the redox properties of V^{IV} interacting species on TiO_2 anatase and rutile samples were further characterized by studying the reactivity of the samples in (i) isothermal (673 K) reduction using a flow of 2% H_2 in helium and (ii) subsequent oxidation (flow of 20% O_2 in nitrogen). The results are reported in Fig. 5. The starting compounds were the samples after long-run catalytic tests (500 h); non-interacting vanadium species were extracted in dilute H_2SO_4 aqueous solution. The results are reported as millimoles of O removed (or acquired) per mg of catalyst in order to show the absolute amounts of weight change (Fig. 5A) and as millimoles of O removed (or acquired) per millimoles of V_2O_4 (1 mmol of O removed corresponds to the reduction of 2 mmol of V^{IV} to V^{III}) (Fig. 5B) in order to show the weight change relative to the vandium content. The results are reported according to the two modalities, because the initial amount of V^{IV} in the two samples (anatase and rutile) after long-term catalytic tests is different (see Table 1) and a large part of the insoluble V^{IV} species in the rutile sample is in the bulk of the solid due to the formation of a solid solution (Table 2) and thus not accessible to redox interaction with H_2 and O_2. Preliminary experiments with pure TiO_2 indicate that reduction of Ti(IV) sites occurs only to a very limited extent in our experimental conditions.

The data clearly illustrate the redox behavior of V^{IV} in the two samples: (i) All vanadium V^{IV} on the anatase surface can be reduced to V^{III} (Fig. 5A) which, in the presence of O_2, is quickly reoxidized to V^{IV}, but not further oxidized to V^{V}; (ii) only about 20% of V^{IV} in the rutile sample can be reduced or reoxidized and, therefore, we may assume that only this part is on the surface and accessible to the molecules involved in reduction/oxidation cycles. Its absolute amount is also lower than that present on the surface of anatase, thus evidencing incomplete surface coverage; (iii) the V^{IV} on the anatase surface cannot be oxidized to V^{V}, the opposite of that observed for V^{IV} on the rutile phase. Figure 5, in fact, clearly shows that in rutile samples after quick oxidation of V^{III} to V^{IV}, oxidation of the latter

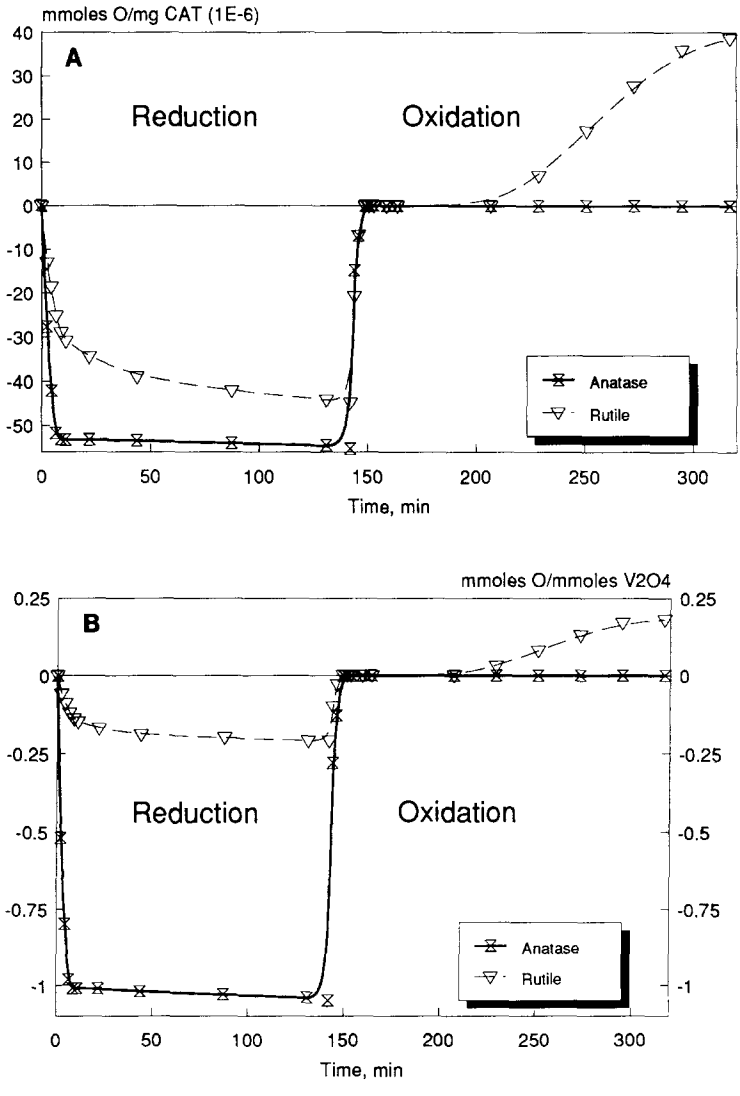

FIG. 5. Isothermal (673 K) reduction (flow of 2% H_2 in helium) and subsequent reoxidation (flow of 20% O_2 in nitrogen) of V_2O_5 and TiO_2 anatase (A) and rutile (R) mixtures after long-term catalytic tests (*o*-xylene oxidation, 500 h) and subsequent extraction (dilute aq. H_2SO_4 solution) of the non-interacting V species. Starting TiO_2 samples were the same as those of Fig. 3.

to V^V begins but takes place at a rate much slower than that of the former reaction.

XPS Characterization

Reported in Table 3 is the characterization by X-ray photoelectron spectroscopy (XPS) of the non-soluble V^{IV} species formed on the surface of titanium oxide by solid-state interaction of V_2O_5 and TiO_2. Soluble V-oxide species are removed before the evacuation of the samples for XPS measurements. The binding energy of $V_{2p_{3/2}}$ peak and the relative full width at half maximum ⟨FWHM⟩ of some reference V-oxide samples have been also reported.

It is known that XPS $V_{2p_{3/2}}$ peak of non-soluble V^{IV} on TiO_2 (anatase) surface well agrees with that expected for a V^{IV} com-

TABLE 3

Characterization by XPS of Non-soluble V^{IV} Species Present on TiO_2 Surface as a Function of the Crystalline Nature of TiO_2

TiO_2 crystalline form	Surface area (m^2/g)	Binding energies[a] (eV)	Full width at half maximum (eV)	Atomic ratio (V/Ti)	Atomic ratio (V/Ti) after removal of about two layers
Anatase	9.8	516.1	3.0	0.043	0.006
Rutile	8.7	516.6	2.6	0.102	0.054

Note. Values of binding energies (eV) of $V_{2p_{3/2}}$ and full width at half maximum (FWHM) (eV) for some reference V-oxides: V_2O_5 517.1 (1.6), V_2O_4 516.0 (3.2), V_6O_{13} 516.6 (2.6), $VOSO_4$ 516.1 (3.0). Charging effect has been corrected using the O_{1s} peak at 529.8 eV as a reference. The sputtering of the surface was realized using a Ne^+ ion gun.

[a] Values of binding energies of $V_{2p_{3/2}}$.

pound. After removal of about two layers by Ne^+ ion gun sputtering the intensity of the signal of vanadium decreases to nearly zero, confirming that all the V^{IV} is localized on the surface. On the contrary, XPS signal in rutile samples suggests the presence of a partial surface oxidation of vanadium and the presence of a mixed valence V^{IV}–V^V compound like V_6O_{13}. The removal of about two layers halves the intensity of the $V_{2p_{3/2}}$ signal, which, however, could be still clearly evidenced. This indicates that non-soluble V^{IV} is not only present on the surface of TiO_2 (rutile), but also in solid solution with it.

ESR Characterization

Anatase samples. The ESR spectra (77 K, vacuum) of a sample prepared by mechanical mixing of 0.8% V_2O_5 with TiO_2 anatase (9.8 m^2/g), calcination at 773 K and subsequent removal of soluble V species by selective extraction is reported in Fig. 6a. The preliminary extraction of the soluble V^V species is fundamental for correct characterization of the V^{IV} interacting species. As previously shown (*21*) the vacuum treatment usually utilized for the pretreatment of ESR samples, in fact, gives rise to partial reduction of V^V species with the formation of additional V^{IV} species that may alter the characterization of the samples. In all the following samples the same extraction procedure was made in order to characterize selectively only the V^{IV} interacting species.

Due to the small amount of the starting V_2O_5 used for the preparation of the sample of Fig. 6a (approximately $\frac{1}{10}$ of that usually utilized) the amount of V^{IV} formed corresponds to about 30–40% of the reference monolayer and thus is much lower than that found using the usual 7.7 wt% of V_2O_5 for the preparation of the samples (near to monolayer). The ESR spectra after outgassing at 473 and 673 K are reported in Figs. 6 a1 and 6 a2, respectively.

The ESR spectrum obtained upon outgassing at 473 K (Fig. 6 a1) shows at least two resolved sets of parallel hyperfine lines due to two V^{IV} species (d^1, $S = \frac{1}{2}$) with their unpaired electron in interaction with the $I = \frac{7}{2}$ nucleus of ^{51}V (100% of natural abundance) (species A and B). The symmetries of the g tensor are axial and, on the basis of the lack of line broadening, the species are thought to be isolated. The spin-Hamiltonian parameters, as deduced taking into account the second-order effects, can be determined for both A and B species only for their parallel part, whose parameters are as follows:

$$\text{A } g_{//} = 1.907 \quad A_{//} = 180\text{–}182 \text{ G}$$

$$\text{B } g_{//} = 1.938 \quad A_{//} = 180\text{–}182 \text{ G}$$

The perpendicular part is not easily observable except for a few lines in the high field region of the spectrum that allow a rough evaluation of g and A which are, for both species, between 1.96 and 1.98 and between 50 and 70 G, respectively. The B species, on the basis of spectrum 6 a1, are slightly more abundant than those of type A. Despite the incomplete resolution, the high value of the isotropic hyperfine coupling constant indicates a relevant asymmetry of the coordination sphere of vanadium(IV), typical of vanadyl (VO^{2+}) complexes (*28*). The large parallel hyperfine coupling constant indicates a probable high ionicity of the in-plane V–O bond. The spectra are sensitive to adsorption of CO and

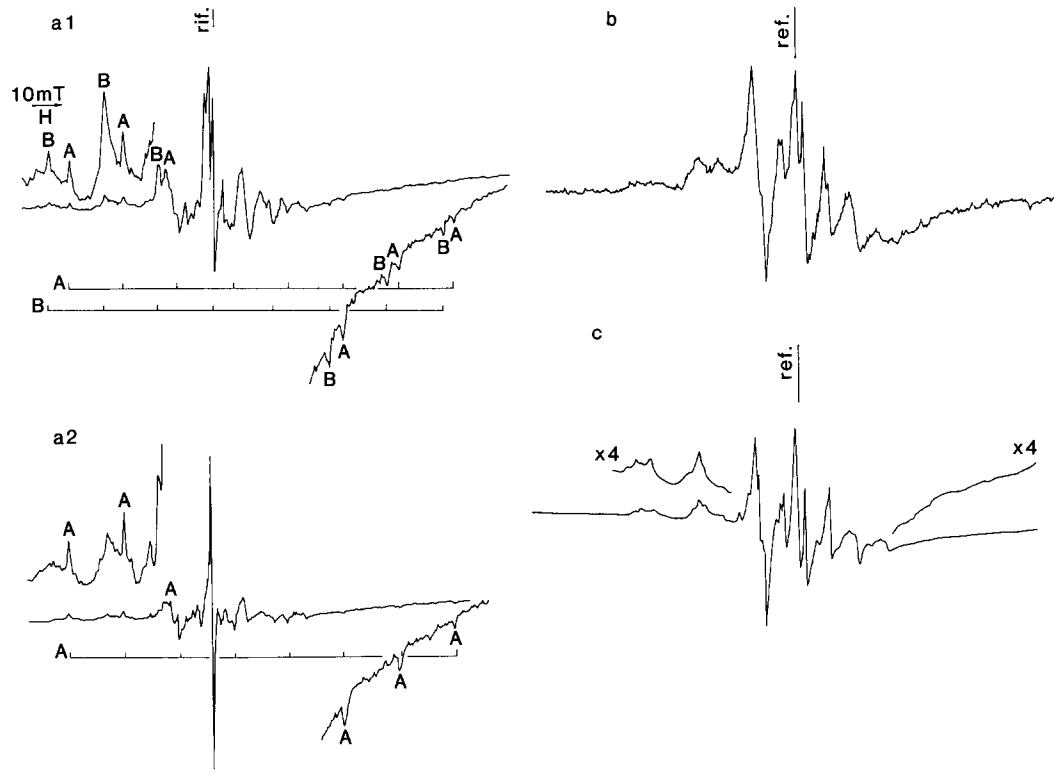

FIG. 6. EPR spectra (77 K, vacuum) of non-soluble V^{IV} in anatase samples. (a) 0.8% V_2O_5/TiO_2 after outgassing at 473 K (*a1*) and at 673 K (*a2*), (b) 7.7% V_2O_5/TiO_2 after outgassing at 673 K, (c) 7.7% V_2O_5/Ti-hydroxygel (see text) after outgassing at 673 K. Gain in the ESR spectra: (*a1*) 4E3, (*a2*) 2E3, (b) 8E2, (c) 4E2. Microwave power = 10 mW.

H_2O and thus may be assigned to coordinatively unsaturated surface isolated vanadyl ions in distorted octahedral or square pyramidal coordination on the basis of the comparison with V^{IV} ESR spectra of V–Ti–O catalysts (*19, 20, 22, 25, 29, 30, 31–34*) and reference samples (*28*). The A species is probably more coordinatively unsaturated than the B species (*37*).

Upon the annealing treatment at 673 K, the profile of the spectrum (Fig. 6 *a2*) is modified as follows:

(i) In the central part of the spectrum, around the free electron g value, a new sharp, symmetric line is present which cannot be ascribed to V^{4+} sites and probably is due to defective centers in the TiO_2.

(ii) An inversion occurs in the abundances of A and B species; the intensity of the former now prevails in the spectrum.

With increasing amounts of V^{IV} interacting species present on the anatase sample, the spectrum decreases progressively in intensity, resolution, and definition. Figure 6b reports the ESR spectrum (77 K, vacuum) obtained for an anatase sample (9.8 m^2/g) prepared using the usual 7.7 wt% of V_2O_5. In this sample, as previously described, the amount of V^{IV} is approximately equivalent to that of the reference monolayer. A dominant structured signal is superimposed on a broad unresolved weak signal centered at about $g = 1.98$. The latter signal is present in slightly reduced vanadium(V) oxide (*35*) and may be assigned to magnetically interacting V^{IV} species. The lower res-

olution of the structured signal may be due, in addition to mutual interaction of neighboring vanadyl species, to the superimposition of several similar structured signals due to the presence of a multiplicity of vanadium sites in slightly different environments. This is confirmed by spectrum 6 *c* of an anatase sample prepared by mechanically mixing V_2O_5 with the hydroxygel precursor of anatase TiO_2, followed by calcination. As previously described, this method allows the formation of a large amount of interacting V^{IV}. The amount of V^{IV} is 1.8%, but due to the higher surface area of the sample, this value corresponds to around 60–70% of the reference monolayer. The features of the ESR spectrum (77 K, vacuum) (Fig. 6c) so obtained perfectly overlap those of the spectrum in Fig. 6b in spite of the lower resolution and the broad unresolved signal present in the latter one. The spectrum may be analyzed as the superimposition of at least five distinct signals all exhibiting hyperfine structure. This is clearly observed in the low-field portion of the spectrum where the $-\frac{7}{2}$ and $-\frac{5}{2}$ parallel components are clearly split into five distinct lines. All signals may be attributed (*28–34*) to the presence of at least five types of isolated vanadyl ions in symmetry of distorted octahedral origin differing in the environment and, most probably, in the coordination number. The spectrum is basically similar to that observed on the low loading V–TiO_2 sample after outgassing at 473 K (Fig. 6 *a1*) notwithstanding the presence of a reduced number of vanadium species in the latter. A contribution to the unusual multiplicity of species may be also attributed to the interaction with different crystalline faces of the TiO_2 anatase surface. Detailed analysis of the different species present is in progress, but at this time it may be suggested that the species are influenced differently by the coordination of probe molecules such as CO, NO, and H_2O (*36*). The lower resolution of spectrum 6 *b* in comparison to spectrum 6 *c* can be attributed to the higher magnetic interaction between neighboring vanadylic groups favored by the lower surface area of the sample and by the onset of the broad unstructured signal due to even more interacting ions. This interaction is reduced in sample c where the surface coverage is below (around 60–70%) that for the reference monolayer, but the absolute amount of V^{IV} sites is nearly equal to that of sample 6b. On the other hand, this indicates that the vanadyl ions on the anatase samples are well dispersed on the surface and that magnetic long-range interaction is present only in samples where surface coverage with interacting V^{IV} is near the reference monolayer.

Rutile samples. A completely different situation is shown by rutile samples (Fig. 7). The ESR spectrum (77 K, vacuum) of the sample after calcination prepared in a way analogous to that for the sample of Fig. 6b, i.e., starting with 7.7 wt% V_2O_5, is shown in Fig. 7a. Superimposed on an intense broad unstructured signal with a g value of about 1.98 characteristic of near-lying V^{IV} paramagnetic centers, a signal is present (signal a1) that exhibits a well-resolved parallel hyperfine structure ($g_{//} = 1.958$, $A_{//} = 153$ G) and a partially hindered perpendicular one whose values seem to be $g_{\perp} \approx 1.96$ and $A_{\perp} \approx 50$ G. A second signal is also observed (signal a2) whose hyperfine structure is visible on the low-field site of the spectrum where it overlaps the hyperfine components of signal a1. The linewidth of a2 is larger than that of a1 and its intensity is definitely lower. The latter cannot be analyzed unambiguously, but may be tentatively attributed to a highly distorted V^{IV} group. The values of the parameters of signal a1 are similar (at least in the parallel part) to those found by Meriaudeau and Vedrine (*30*) and Gallay *et al.* (*29*) and assigned to non-vanadylic V^{4+} sites in substitutional position in the rutile structure. More recently a similar spectrum was assigned to V^{4+} sites in a phase of poorly crystalline rutile (*37*). The presence of signal a2 may be confirmed in the analysis of a rutile sample prepared in a way analogous to that for the sample of Fig. 6c in which the preparation leads to an increased

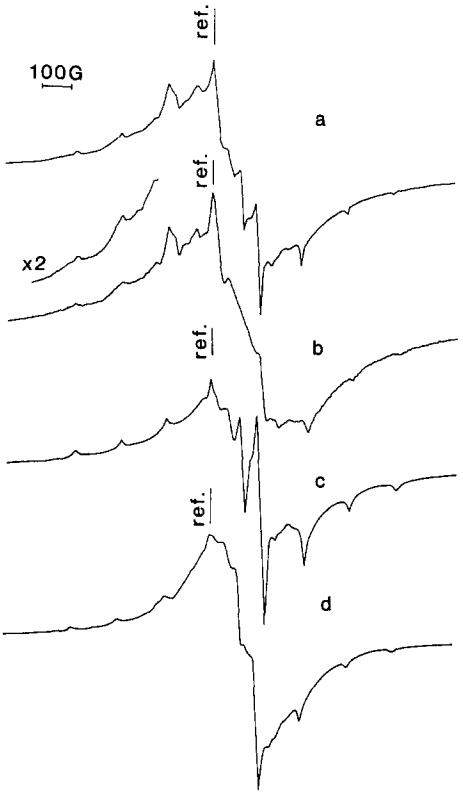

FIG. 7. EPR spectra (77 K, vacuum) of non-soluble V^{IV} in rutile samples. All samples were outgassed at 673 K. (a) 7.7% V_2O_5/TiO_2, (b) 7.7% V_2O_5/Ti-hydroxygel (see text), (c) sample a after catalytic tests in *o*-xylene oxidation (5 h), (d) 7.7% V_2O_5/TiO_2 after catalytic tests in *o*-xylene oxidation (more than 500 h). Gain in the ESR spectra: (a) 8E2, (b) 2E2, (c) 2.5E2, (d) 3.2E2.

amount of interacting V^{IV} species and to a higher surface area (around 20 m^2/g). The ESR spectrum (77 K, vacuum) of this sample (Fig. 7b) is similar to that of the sample of Fig. 7a, but the relative intensity of signal a2 with respect to signal a1 (assigned to V^{IV} in solid solution) is slightly increased. This suggests the possibility that the a1 species may be related to near surface sites in a distorted environment. The ESR parameters that may be tentatively estimated from the spectrum are intermediate between those of surface VO^{2+} sites such as those in anatase (Fig. 6) and those of substitutional V^{4+} sites in rutile, even though the parameters cannot be unambiguously estimated. For anatase samples, the use of low amounts of V_2O_5 in the starting mixture in order to evidence some V^{IV} species more clearly (compare Figs. 6a and 6b), on the contrary, does not give appreciable results; only a weak broad signal due to strongly magnetically interacting species is observed.

The nature of signal a2 is confirmed by the ESR spectrum of the sample of Fig. 7a recorded after catalytic tests in *o*-xylene oxidation (Fig. 7c). The spectrum clearly evidences the presence of only the broad unstructured signal superimposed to signal a1. During the catalytic tests, therefore, species a2 disappears, in agreement with tentative attribution to a near-surface-distorted V(IV) species and to the results of time-on-stream catalytic tests.

The ESR spectrum of a rutile sample that has worked for a longer time (more than 500 h) in *o*-xylene oxidation before the washing procedure is shown in Fig. 7d. The spectrum is similar to that observed previously. The spectrum derives from the superimposition of an intense broad signal on the weak signal a1 and possibly on the second signal with hyperfine structure called a2.

DISCUSSION

The presence of V^{IV} sites in $V-TiO_2$ (anatase) catalysts is usually considered negligible in the literature and mainly attributed (i) to the presence of some residual or adsorbed reagent such as ammonia or oxalic acid that may cause partial reduction of the catalyst during calcination or (ii) to a partial phase transformation of titania with formation of a rutile $V^{IV}-TiO_2$ solid solution.

The results of this work, on the contrary, evidence the following aspects.

(a) There is a specific reaction of V^V ions with the TiO_2 (anatase) surface with formation of V^{IV} surface sites even in aerobic conditions and the absence of any reducing agent or long-range phase transformation to TiO_2 (rutile).

(b) The formation of V^{IV} sites is not negli-

gible and in low surface area samples, their amount reaches a value nearly equal to that of the theoretical reference monolayer.

(c) These surface V^{IV} sites can be reduced to V^{III}, but cannot be oxidized to V^{V} due to specific interaction with titania and thus exhibit different redox properties than other vanadium-oxide supported species.

(d) The formation of these V^{IV} interacting species influences the reactivity of the titania surface. The V^{IV}-modified TiO_2 surface is active in *o*-xylene oxidation, although the selectivity is relatively low. The selectivity improves when oxidation to V^{V} occurs, such as in the rutile sample.

The characterization of similar catalysts reported in the literature is usually performed before the catalytic tests and by means of physical techniques that do not allow a clear and quantitative detection of the nature, amount, and distribution of V^{IV} sites in the catalyst. Better information can be obtained by using the technique of multiple titration combined with selective extraction as done in the present work. Our results, therefore, are not directly comparable with literature data, but do suggest that the formation of V^{IV} interacting species is a more general phenomenon of the surface chemistry and reactivity of V-oxide on titania, not specifically related to our method of preparation. In fact, V^{IV} forms by calcination and solid-state interaction between the V_2O_5 and TiO_2 oxides. It is thus reasonable to assume that V^{IV} is present also in catalysts prepared by other methods or possibly may form during catalytic testing.

Genesis of Interacting V^{IV} Sites on TiO_2 (Anatase) Surface

The method of preparation by solid-state reaction of V_2O_5 and TiO_2 evidences that the genesis of V^{IV} interacting sites derives from the reaction of V^{V} ions with specific sites of the TiO_2 (anatase) surface. The driving force of the reaction is sufficient to allow the spontaneous reduction of vanadium with the formation of stable VO^{2+} sites during calcination.

The results of the tests using different atmospheres for heating V_2O_5/TiO_2 solid-state mixtures and using the oxyhydrate precursor of the TiO_2 (anatase) suggest that the formation of V^{IV} interacting sites derives from the surface reaction of condensation of Ti–OH groups with isolated "mobile" vanadate (V^{V}) groups. In fact, the amount of V^{IV} interacting sites on low surface area TiO_2 (anatase) is nearly equal to the reference monolayer. The ESR spectrum (Fig. 6c) shows the prevalent presence of V^{IV} sites with a non-negligible degree of mutual interaction. These V^{IV} interacting sites are on the surface, since they are easily accessible to gaseous molecules as shown by reduction/reoxidation experiments (Fig. 5) and as also confirmed by ESR experiments with different probe molecules (*36*). All these indications therefore suggest homogeneous spreading of V^{IV} interacting sites on low surface area TiO_2 (anatase) samples.

This requires that isolated V^{V} species diffuse on the hydroxylated titania surface giving rise to a homogeneous distribution of V^{IV} sites on the entire surface. In fact, tests on low surface area TiO_2 samples where (a) the TiO_2/V_2O_5 relative weight ratio is decreased from about 13 (as that utilized in this work) to 1 (drastic increase in the relative amount of V_2O_5) and (b) the dimensions of the TiO_2 and V_2O_5 particles are reduced by grinding before the mixing do not provide evidence for an increase in the amount of V^{IV} interacting species. This suggests that the amount of interacting V^{IV} formed does not depend on the area of contact of the V_2O_5 and TiO_2 grains. The V^{IV} forms not only at the interface between the two phases, but also on the entire titania surface. This implies that the V^{V}, at temperatures around 723 K, has a sufficient surface diffusion to allow homogeneous spreading, in agreement with literature indications (*5* and references therein).

We may observe that the vanadium probably diffuses as mononuclear vanadate species such as $[H_2VO_4]^-$ according to (a) the formation of isolated V^{IV} interacting species and (b) the phase diagram of vana-

dium species in solution (*38*), taking into account the surface acidity of pure titania (*39*) and also the presence at high temperatures of strongly adsorbed molecular water on specific crystallographic faces of TiO_2 (*40*). This adsorbed layer may constitute the medium for surface diffusion of vanadium species, in agreement also with the mechanism of intraparticle diffusion into zeolitic cavities hypothesized for the solid-state interaction of transition metal oxides with zeolites (*41*).

This mechanism of surface diffusion is in agreement with the evidence that (a) as the surface area of the TiO_2 sample increases the relative fraction of interacting V^{IV} with respect to the reference monolayer decreases and (b) increasing the water partial pressure during calcination increases the amount of interacting V^{IV}, especially in high surface area samples.

The (001) crystallographic plane is the principal one exposed on the surface of low surface area (around 5–10 m^2/g) anatase samples, whereas different crystallographic faces become predominant in samples with higher surface areas (*39, 40*) with a decrease in the relative fraction of the surface covered by a strongly adsorbed layer of molecular water (*40*). On the low surface area samples the preferential reaction of vanadium is thus with sites on this crystallographic plane, whereas for higher surface area samples the reaction may also occur on other crystallographic planes. This is in agreement with the difference in the ESR spectra of samples with different surface areas (compare spectra 6 *a1* and 6 *c*).

The mechanism of genesis of these V^{IV} species may thus be tentatively schematized as follows:

(a) hydrolysis of V_2O_5 particles at the V_2O_5/TiO_2 interface;

(b) surface diffusion of isolated vanadate species through a medium of a possibly strongly adsorbed water-like layer;

(c) reaction of V^V species with titanium sites with generation of stable VO^{2+} isolated surface groups.

The reason for the reduction of V^V to V^{IV} induced by reaction with the titania surface is not clear. This may be related to better stabilization of surface V^{IV} (d^1) distorted octahedral or square-pyramidal complexes with O ligands in comparison to analogous V^V (d^0) complexes (*43*) due to better orbital overlap of oxygen (strong π donor character) atoms with a transition metal having *d* electrons. Alternatively, during high-temperature calcination there is dehydroxylation of OH surface sites with the formation of Ti^{3+} sites and oxygen vacancies and evolution of gaseous O_2 (*42*). The Ti^{3+} sites react with V^{5+} forming Ti^{4+} and V^{4+}. The formation of defective centers in TiO_2 upon outgassing (Fig. 6 *a2*) is in agreement with this type of hypothesis of mechanism.

We cannot ignore the fact that the formation of V^{IV} interacting sites may also give rise to a surface rearrangement of TiO_2 octahedra which can also explain the observed stabilization of V^{IV} sites. This transformation, if any, is confined to the first layers only. In fact no structural (XRD, IR), physicochemical and reactivity (see below) evidence was found regarding the formation of a long-range rutile-type order and structure. Moreover, the constancy of the detected amount of V^{IV} in the catalysts calcined at different temperature and for different times, the EPR data and the redox characteristics of rutile and anatase samples suggest that the formation of V^{IV} probably does not involve a rearrangement of the TiO_2 surface, but is due only to the preferential stabilization of its surface complexes. This also can explain why the amount of the non-soluble V^{IV} formed is not affected by the presence of a large amount of V^{IV} generated, for example, by reduction of the crystalline V_2O_5 by a reducing agent.

Model of the TiO_2 (Anatase) Surface Modified by V^{IV} Sites

The available information about the nature of surface V^{IV} interacting sites may be summarized as follows.

ESR spectroscopy evidences the presence on the surface of TiO_2 (anatase) of sev-

eral isolated vanadyl species likely in distorted octahedral or square-pyramidal coordination. The differences between the species are mainly related to different coordinative unsaturated situations or environments (*36*). Some of these species may interconvert from one to the other when suitable basic probe molecules are added (*36*), thus indicating the presence of Lewis acidity, in agreement with FT–IR characterization of V-modified titania surfaces (*19, 20*). FT–IR characterization also provides evidence (*19, 20*) about the presence of Brønsted acidity related to V–OH groups. It should be noted that these FT–IR data were obtained using high surface area samples, whereas FT–IR characterization of surface acidity is not possible in low surface area samples, due to excessive light scattering. We may, however, hypothesize that V–OH sites are also present in low surface area samples, in agreement with the activity of the V^{IV}-modified TiO_2 surface in hydrocarbon isomerization.

ESR analysis also shows that in a sample where the amount of V^{IV} is nearly equal to the reference monolayer (Fig. 6) a large fraction of isolated VO^{2+} groups is present that show only weak mutual magnetic interaction. This suggests that these VO^{2+} sites do not share neighboring surface TiO_2 lattice oxygens and also do not share other oxygen atoms forming surface polyoxoanions.

We also assume that the [001] plane is the predominant crystallographic plane exposed on the surface of low surface area (around 10 m^2/g) TiO_2 (anatase) (*39*).

A model of the surface of V^{IV}-modified TiO_2 (anatase) that fit the previous observations is shown schematically in Fig. 8, where full, dotted, and hatched circles indicate Ti–O–V shared oxygens, Ti–O···V weak interacting oxygen and V–O···H···O–Ti H-bonded oxygens of the TiO_2 lattice, respectively. Open circles indicate oxygen atoms in the TiO_2 lattice, which do not interact directly with vanadium units, and small circles indicate Ti or V atoms. It should be noted that the surface coverage estimated by this model agrees well with the maximum value found for V^{IV} interacting species per square meter of the TiO_2 surface area (Fig. 1), which indicates a mean V to V distance of about 4.5 Å based on a homogeneous distribution of vanadium sites. Also reported in Fig. 8 is an example of the possible localization of V^{IV} sites on other crystallographic planes of TiO_2 (anatase), which indicates the presence of different coordination environments for the V^{IV} sites based on ESR indications.

Finally, it is important to remark that the V^{IV} layer interacting with the TiO_2 surface is indeed something different from what is related as a monolayer in literature. The latter is thought to be a homogeneously dispersed V^V phase responsible for the selective oxidation of the *o*-xylene. This topic is discussed in the second part of the paper.

Reactivity of the V^{IV}-Modified TiO_2 Surface

The tests of surface reactivity in *o*-xylene oxidation (Fig. 3) clearly show a considerable increase in the rate of *o*-xylene activation, but the value of selectivity to phthalic anhydride observed is much below that of the V^V-covered TiO_2 surface. This is indication that the presence of V^{IV} on the surface (if not upper V^V sites are present) alters the reactivity and causes a loss of selectivity in active catalysts. However, we may also speculate that the V^{IV} sites may play a role in the activation of *o*-xylene while V^V sites are involved mainly in the stage of oxygen insertion on the activated hydrocarbon (*18*).

The evidence of a certain selectivity to phthalic anhydride on the titania surface modified by interacting V^{IV} also suggests that stable V^{IV} sites are able to activate adsorbed oxygen species without being oxidized to V^V. These oxygen species are relatively selective in *o*-xylene transformation to phthalic anhydride, but may be more selective in other reactions of selective oxidation for which lattice oxygen may be less useful, namely in some reactions of alkane selective transformation. However, both the importance of V^{IV} sites in the mechanism of *o*-xylene transformation and the role

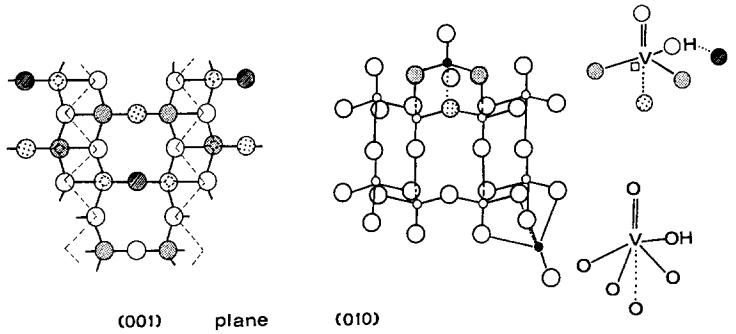

FIG. 8. Model of the surface of a non-soluble V^{IV}-modified low surface area TiO_2 (anatase) sample: (001) and 010) crystallographic planes. Full, dotted, and hatched circles indicate Ti–O–V shared oxygens, Ti–O···V weak interacting oxygens and V–O···H···O–Ti H-bonded oxygens in the TiO_2 lattice, respectively. Open circles indicate oxygens of the TiO_2 lattice which do not interact directly with vanadium units and small circles indicate Ti or V atoms.

of V^{IV} in creating oxygen adspecies require more detailed studies.

Differences between V^{IV} Sites on Anatase and Rutile TiO_2

The differences in the situation with respect to the V^{IV} sites in TiO_2 (rutile) samples as compared with TiO_2 (anatase) samples can be summarized as follows:

(a) Possibility of the formation of a solid solution (Tables 2, 3) and of amounts of V^{IV} up to 3–4 times greater than the reference monolayer (Fig. 1).

(b) Considerable increase in the amount of V^{IV} with reducing treatments (Fig. 1).

(c) Redox properties and in particular the possibility of oxidation of V^{IV} to V^{V} and the lower amount of V^{IV} sites accessible to reduction/reoxidation (Fig. 5).

(d) Evolution of the surface reactivity as a function of time in the reactive environment and of the amount of V^{IV} sites in the sample (Fig. 4).

(e) Completely different ESR spectra (Fig. 7) with the presence mainly of magnetically interacting V^{IV} species even in samples with a low surface coverage and substituted V^{IV} sites in the rutile phase.

(f) A slightly different XPS $V_{2p_{3/2}}$ peak (Table 3) and an especially different depth profile, indicating the surface localization of non-soluble V^{IV} sites in anatase sample and also the presence of a solid solution in rutile sample.

These observations can be explained by considering that in rutile there is competition between surface diffusion of vanadium species and bulk diffusion, with the formation of the substitutional solid solution. The prevalence of the latter effect with respect to the former probably causes the localization of the formation of V^{IV} species at the interface between grains of TiO_2 and V_2O_5 with the formation of rutile V_2O_4-like islands coherently intergrown in the main rutile TiO_2 matrix. This model may explain (i) the observed ESR and XPS data, (ii) the insolubility of these islands in dilute H_2SO_4 solution, and (iii) the slower rate of oxidation to V^{V} in comparison with other supported V^{IV}-containing species which are soluble in the extraction medium and show much higher rates of oxidation.

Only when the amount of V^{IV} in the rutile intergrowth structure is near the limiting value (near 4 wt% as equivalent V_2O_5 according to our results) is diffusion toward the bulk of the sample avoided and the V^{IV} tends to be reoxidized to V^{V} with an increase in the catalytic behavior (Fig. 4, sample d).

On the contrary, in samples with lower amounts of V^{IV}, the effect of diffusion toward the bulk prevails over oxidation with a progressive worsening of the catalytic behavior (Fig. 4, sample c).

REFERENCES

1. Wachs, I. E., Saleh, R. Y., Chan, S. S., and Chersich, C. C., *Appl. Catal.* **15,** 339 (1985).
2. Saleh, R. Y., Wachs, I. E., Chan, S. S., and Chersich, C. C., *J. Catal.* **98,** 102 (1986).
3. Bond, G. C., and König, P., *J. Catal.* **77,** 309 (1982).
4. Bond, G. C., and Brückman, K., *Faraday Discuss. Chem. Soc.* **72,** 235 (1982).
5. Bond, G. C., Flamerz, S., and Shukri, R., *Faraday Discuss. Chem. Soc.* **87,** 65 (1989).
6. Vejux, A., and Courtine, P., *J. Solid State Chem.* **23,** 93 (1978).
7. Vejux, A., and Courtine, P., *C.R. Acad. Sci. Ser. C* **286,** 135 (1978).
8. Gasior, M., and Machej, T., *J. Catal.* **83,** 472 (1983).
9. Kang, Z. C., and Bao, Q. X., *Appl. Catal.* **26,** 251 (1986).
10. Nakagawa, Y., Ono, T., Miyata, H., and Kubokawa, Y., *J. Chem. Soc. Faraday Trans. 1* **79,** 2929 (1983).
11. Inomata, M., Mori, K., Miyamoto, A., Ui, T., and Murakami, Y., *J. Phys. Chem.* **87,** 754 (1983).
12. Miyamoto, A., Mori, K., Inomata, M., and Murakami, Y., *in* "Proceedings, 8th International Congress on Catalysis, Berlin, 1984," Vol. 4, p. 285. Dechema, Frankfurt-am-Main, 1984.
13. Baiker, A., Dollenmeier, P., Glinski, M., and Reller, A., *Appl. Catal.* **35,** 351 (1987).
14. Bond, G. C., Zurita, J. P., and Flamerz, S., *Appl. Catal.* **27,** 353 (1986).
15. Hausinger, H., Schmelz, H., and Knözinger, H., *Appl. Catal.* **39,** 267 (1988).
16. Kozlowski, R., Pettifer, R. F., and Thomas, J. M., *J. Phys. Chem.*, **87,** 5176 (1983).
17. Haber, J., Kozlowska, A., and Kozlowski, R., *J. Catal.* **102,** 52 (1986).
18. Cavani, F., Centi, G., Parrinello, F., and Trifiro', F., *in* "Preparation of Catalysts IV" (B. Delmon, P. Grange, P. A. Jacobs, and G. Poncelet, Eds.), p. 227. Elsevier, Amsterdam, 1987.
19. Busca, G., Marchetti, L., Centi, G., and Trifiro', F., *J. Chem. Soc. Faraday Trans. 1* **81,** 1003 (1985).
20. Busca, G., Marchetti, L., Centi, G., and Trifiro', F., *Langmuir* **2,** 568 (1986).
21. Centi, G., Pinelli, D., and Trifiro', F., *J. Mol. Catal.* **59,** 221 (1990).
22. Cavani, F., Centi, G., Foresti, E., Trifiro', F., and Busca, G., *J. Chem. Soc. Faraday Trans. 1* **84,** 237 (1988).
23. Busca, G., Cavani, F., Foresti, E., and Trifiro', F., *J. Catal.* **106,** 251 (1987).
24. Fierro, J. L. G., Arrua, L. A., Lopez Nieto, J. M., and Kremenic, G., *Appl. Catal.* **37,** 323 (1988).
25. Risiecka, M., Grzybowska, B., and Gasior, M., *Appl. Catal.* **10,** 101 (1984).
26. U. K. Patent 4385496, Assigned to Wacker Chemie, 1972.
27. Cavani, F., Foresti, E., Parrinello, F., and Trifiro', F., *Appl. Catal.* **38,** 311 (1988).
28. Selbin, J., *Chem. Rev.* **65,** 135 (1965).
29. Gallay, R., van der Klink, J. J., and Moser, *J. Phys. Rev. B* **34,** 3060 (1986).
30. Meriaudeau, P., and Vedrine, J. C., *Nouv. J. Chim.* **2,** 133 (1977).
31. Siegel, I. *Phys. Rev. A* **134,** 193 (1964).
32. Ballhausen, C. J., and Gray, H. B., *Inorg. Chem.* **1,** 111 (1962).
33. Bramman, C. J., Lund, T., Raynor, J. B., and Willis, C. S., *J. Chem. Soc. Dalton* 45 (1975).
34. Guzy, C. M., Raynor, J. B., and Symons, M. C. R., *J. Chem. Soc. A* 2791 (1969).
35. Bielanski, A., Dyrek, K., and Serwicka, E., *J. Catal.* **66,** 316 (1980).
36. Centi, G., Giamello, E., Pinelli, D., and Trifiró, F., manuscript in preparation.
37. Busca, G., and Giamello, E. *Mat. Chem. Phys.* **25,** 475 (1990).
38. Pope, M. T., and Dale, B. W., *Quart. Rev.* **22,** 527 (1968).
39. Busca, G., Saussey, H., Saur, O., Lavalley, J. C., and Lorenzelli, V. *Appl. Catal.* **14,** 245 (1985).
40. Morishige, K., Kanno, F., Ogawara, S., and Sasaki, S., *J. Phys. Chem.* **89,** 4404 (1985).
41. (a) Kucherov, A. V., and Slinkin, A. A., *Zeolites,* **8,** 110 (1988); (b) Kucherov, A. V., Slinkin, A. A., Beyer, G. K., and Borbely, G., *J. Chem. Soc. Faraday Trans. 1* **85,** 2737 (1989).
42. Munuera, G., Gonzalez-Elipe, A. R., Rives-Arnau, V., Navio, A., Malet, P., Soria, J., Conesa, J. C., and Sanz, J., *in "Adsorption and Catalysis on Oxide Surfaces"* (M. Che and G. C. Bond, Eds.), p. 113. Elsevier, Amsterdam, 1985.
43. Wilkinson, G., "Advanced Inorganic Chemistry, 3rd ed. Interscience, New York, 1972.